Hindawi
BioMed Research International
Volume 2020, Article ID 7894712, 9 pages
https://doi.org/10.1155/2020/7894712

Research Article

17-Allylamino-demethoxygeldanamycin Used Alone or in Combination with Sodium Orthovanadate Promotes Apoptosis and Inhibits Invasion of SH-SY5Y Cells by Modulating PIWIL2

Xiaohong Tian,[1] **Wumei Wei**,[1] **Xiaohong Wang**,[1] **Qiang Ao**,[2] **Jun Fan**,[1] **Weijian Hou**,[1] **Shuling Bai**,[1] **and Hao Tong**[1]

[1]*Department of Tissue Engineering, School of Fundamental Science, China Medical University, Shenyang, Liaoning 110122, China*
[2]*Institute of Regulatory Science for Medical Device, National Engineering Research Center for Biomaterials, Sichuan University, Chengdu 610064, China*

Correspondence should be addressed to Xiaohong Tian; 511292011@qq.com

Received 22 June 2020; Revised 27 October 2020; Accepted 5 November 2020; Published 21 November 2020

Academic Editor: Ali Imran

Neuroblastoma (NB) is one of the most common extracranial solid tumors of childhood and accounts for 15% of cancer deaths. Even with the multimodality treatment protocols, the advanced-stage tumor overall 5-year survival rate is less than 50%. Therefore, novel drug therapy targeting cellular signal transduction pathways regulating the apoptotic cascade may be important for the treatment of drug-resistant NB. In our previous studies, we have demonstrated that 5 μM sodium orthovanadate (SOV) induced the apoptosis of SH-SY5Y cells. 17-Allylamino-demethoxygeldanamycin (17-AAG) is a geldanamycin- (GA-) derived heat shock protein 90 (Hsp90) inhibitor, and it has been shown to have potent antitumor activity in head and neck cancers. However, the effect of 17-AAG on the apoptosis of NB cells has not been reported. Therefore, the purpose of this study was to determine the effects of 17-AAG and SOV on the growth and invasion of SH-SY5Y cells in vitro and explore the related mechanism. In this study, we first investigated the antiviability effect of 17-AAG on SH-SY5Y cells, then studied the cell apoptosis and invasion influenced by 17-AAG and SOV, and assessed the role of PIWI-Like2 (PIWIL2) and piRNA-PIWI signaling in it. The results showed that 5 μM 17-AAG inhibited cell growth and viability and induced apoptosis in SH-SY5Y cells. Both 17-AAG and SOV reduced the level of PIWIL2 and Bcl-xl proteins and inhibited the invasion of SH-SY5Y cells. In addition, the combined use of the two drugs had greater effect than the single use of any drug.

1. Introduction

Neuroblastoma (NB) is one of the most common extracranial solid tumors of childhood and accounts for 15% of cancer deaths [1–3]. Even with the multimodality treatment protocols, including chemotherapy, surgery, radiation therapy, and immunotherapy, the advanced-stage tumor overall 5-year survival rate is less than 50% [4–6]. Cases of high-risk NB are associated with frequent relapses and tumors that are resistant to alternative chemotherapy regimens. It is reported that the altered cellular responses to apoptosis are thought to play an important role in drug resistance in high-risk NB [7]. Therefore, novel drug therapy targeting cellular signal transduction pathways regulating the apoptotic cascade may be important for the treatment of drug-resistant NB.

The human NB cell line SH-SY5Y is a commonly used cell line in studies related to NB [8, 9] and neurodegenerative disease, such as Alzheimer's disease (AD) [10] and Parkinson's disease (PD) [11, 12]. For example, SH-SY5Y cells were usually used as a model system in vitro to investigate the effect and mechanism of new drugs and provide a basis for the formulation of drug strategy and the treatment of diseases. Here, we focus on the treatment of NB and study the effect of 17-allylamino-demethoxygeldanamycin (17-AAG) and sodium orthovanadate (SOV, molecular formula: Na_3VO_4) on the apoptosis and invasion of SH-SY5Y cells.

AAG is a geldanamycin- (GA-) derived heat shock protein 90 (Hsp90) inhibitor, which is a less toxic and more stable analog of GA [13]. Hsp90, a ubiquitous chaperone protein, plays significant roles in the organization and maturation of client proteins involved in the progression and survival of tumor cells and has become a therapeutic target for cancer treatment. 17-AAG binds to Hsp90, destroys the Hsp90-client protein cycle, and results in the degradation of Hsp90's client proteins. Several preclinical and clinical studies demonstrated that 17-AAG as a single agent or in combination with other anticancer agents has potent antitumor activity in a range of human cancers [14–17]. However, it has not been reported whether 17-AAG can induce apoptosis of NB cells or not.

SOV is a proverbial vanadium compound and has many biological activities [7]. Many studies have shown that SOV displays antineoplastic activities against various types of cancers, such as hepatocellular carcinoma [18, 19], anaplastic thyroid carcinoma [20], oral squamous cell carcinoma [21], EGFR-mutated lung adenocarcinoma [22], and other tumors [23, 24]. In addition, SOV also has neuroprotective and antidiabetic effects [25, 26]. In our previous study, we have demonstrated that 5 μM SOV induced the apoptosis of SH-SY5Y cells [27]. The results suggested that SOV could be a promising agent to treat the central nervous system tumors.

Multiple studies have shown that the combined use of 17-AAG and other antitumor reagents enhanced its antitumor efficacy. As an antitumor agent, can SOV combined with 17-AAG inhibit tumor development to a greater extent? Therefore, on the basis of previous studies, we also used SH-SY5Y cells as a cell model for relevant studies. Furthermore, studies have shown that SOV can play an antitumor role by inhibiting the piRNA-PIWI signaling pathway [28, 29], so we want to know whether SOV and 17-AAG can inhibit the proliferation and invasion of SH-SY5Y by inhibiting PIWI protein-related signaling pathways.

In this study, we mainly investigated the role of 17-AAG alone or combined with SOV in inhibiting the viability and invasion of SH-SY5Y cells and also explored the potential mechanism of action.

2. Materials and Methods

2.1. Materials and Reagents. The human NB SH-SY5Y cell line was purchased from the Cell Bank of Chinese Academy of Sciences (Cat. No.: SCSP-5014, Shanghai, China). The cells were resuspended and plated on a 10 cm petri dish with Dulbecco's modified Eagle's medium (DMEM; Hyclone), supplemented with 10% fetal bovine serum (FBS; Gibco), 100 U/ml penicillin, and 100 μg/ml streptomycin (Sigma Chemical Co., St. Louis, Missouri), and were grown in a 5% CO_2 incubator at 37°C. After culturing for 72 h, the nonadherent cells were removed. The plastic-adherent cells were treated with 0.25% trypsin containing 1 mM EDTA and passaged when they reached about 90% confluent density and subcultured continuously.

2.2. Cellular Viability Assay. Cellular viability was assessed by an MTT assay (Sigma, USA). In this method, SH-SY5Y cells were seeded in 96-well culture plates at a density of 2000 cells/well in triplicates and subsequently treated with different concentrations (0, 0.001, 0.01, 0.1, 1, 5, 10, and 25 μM) of 17-AAG (Sigma, USA) for 24, 48, 72 h, or 96 h. Control cells were treated with an equal amount of DMSO in culture medium. After treatment, the cells were incubated with a 20 μl MTT reagent (5 mg/ml) for 4 h, and then, the supernatant was discarded and 150 μl DMSO was added, followed by colorimetric analysis using a multilabel plate reader (Bio-Rad) at 490 nm. Cell viability was measured relative to untreated cells at each time point. The formula is as follows: Cell viability (%) = (A490 of experimental group − A490 of blank group)/(A490 of control group − A490 of blank group) × 100%. Data are presented as the mean ± standard errors from independent experiments.

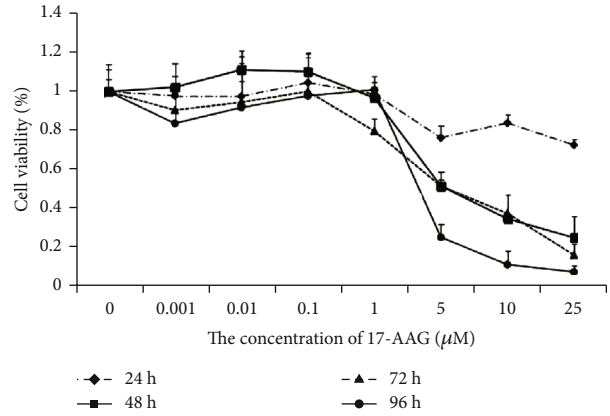

Figure 1: The cell viability of SH-SY5Y cells after 17-AAG treatment at 24 h, 48 h, 72 h, and 96 h ($n = 3$). $P < 0.05$.

2.3. Count and Viability Testing. The quantitative analysis of cell count and viability were obtained using the Muse™ Count & Viability Kit (MCH100102, Merck KGaA, Darmstadt, Germany) on the Muse™ Cell Analyzer (Millipore Corporation, USA). The Muse™ Count & Viability Reagent differently stains viable and dead cells based on their permeability to the two DNA binding dyes present in the reagent. First, 1×10^6 of SH-SY5Y cells were treated with 5 μM 17-AAG or DMSO for 24, 48, 72, or 96 h and then were stained with 450 μl Muse™ Count & Viability Reagent in a sample tube for at least 5 minutes. Finally, the samples were detected by the Muse™ Cell Analyzer according to the manufacturer's instructions. The Muse™ Count & Viability Software Module then performs calculations automatically and displays data in two dot plots.

2.4. Western Blot. 5×10^5 of SH-SY5Y cells were planted on 10 cm dishes and treated with PBS, 5 μM 17-AAG, 5 μM SOV (Sigma-Aldrich), or the mixture of 5 μM (17-AAG +SOV) for 72 h. Then, the cells were lysed with RIPA buffer, and protein concentrations were estimated using the BCA Protein Assay Kit (Thermo Scientific, Rockford, IL). Equal amounts of protein (40 μg) were used for Western blot analysis with antibodies to anti-PIWIL2 (Bioss, bs-3817R) and anti-Bcl-xl (ABclonal, A0209). Specific antibody binding

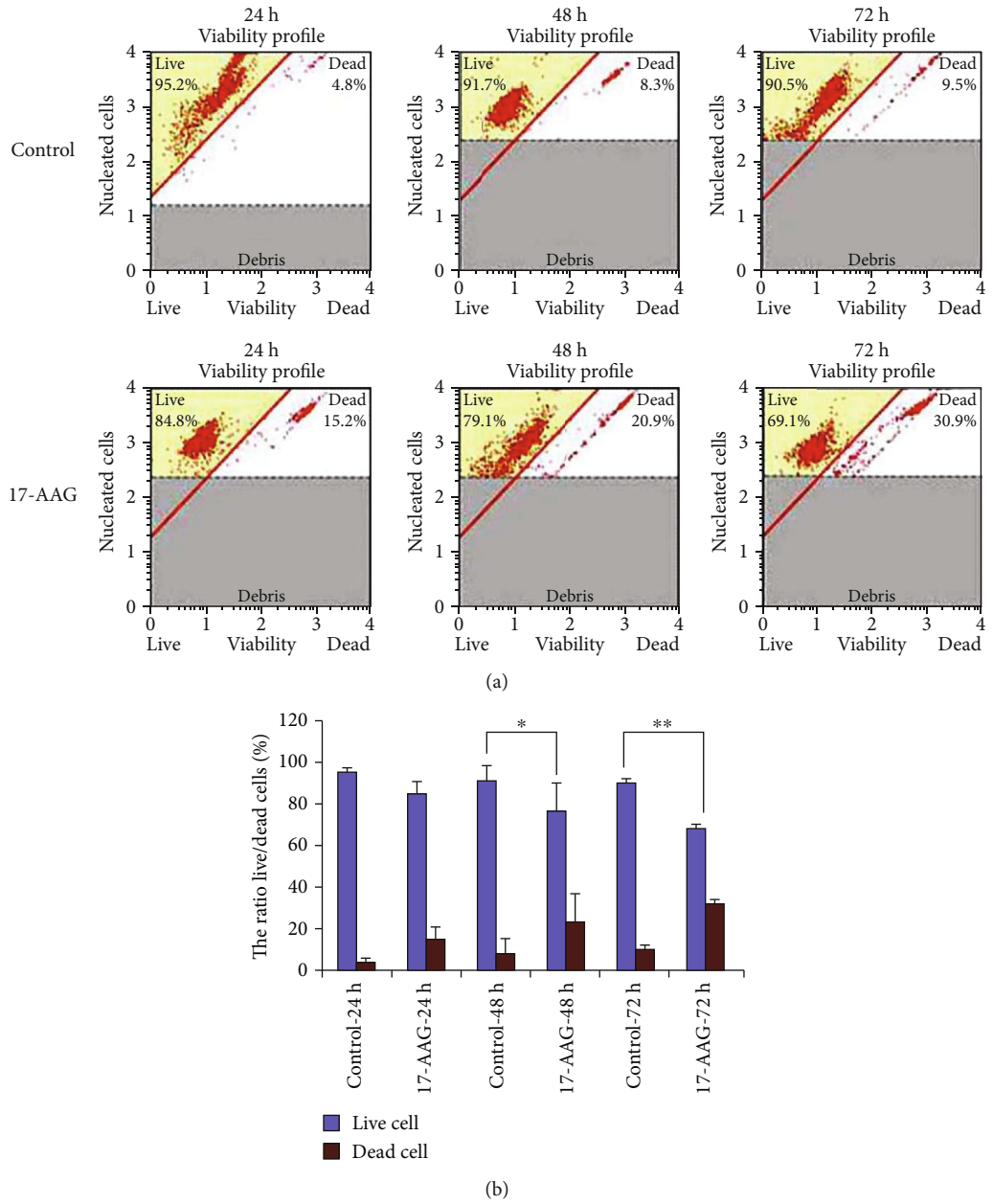

FIGURE 2: 5 μM 17-AAG reduces the percentage of viable cells at 24, 48, and 72 h. (a) The flow chart of SH-SY5Y cells in the control group and 17-AAG group. The viable cells are located in the top left, and dead cells are located in the lower right. (b) The bar graph of the average percent of viable cells and dead cells in the control group and 17-AAG group ($n = 3$, $^{*}P < 0.05$, $^{**}P < 0.01$).

was detected by horseradish peroxidase-conjugated goat anti-rabbit antibodies (Santa Cruz) and visualized with the ECL reagent (Santa Cruz) according to the manufacturer's protocol. Antibody to β-actin was used to evaluate protein loading in each lane.

2.5. Apoptosis Assays. Apoptotic cell death was assessed by the Annexin V-FITC Apoptosis Detection kit (KeyGen Biotech, Nanjing, China) according to the manufacturer's instructions. Firstly, 1×10^5 of SH-SY5Y cells were seeded in 6-well plates, treated with PBS, 5 μM 17-AAG, 5 μM SOV, and the mixture of 5 μM (17-AAG+SOV) for 24, 48, or 72 h, then were double-stained with Annexin V-FITC solution and PI/RNase solution in the dark. Then, each sample was analyzed by FACSort flow cytometry (BD, San Jose, CA, USA). The percentages of cells staining positive for Annexin V were calculated, and means as well as standard error were plotted. Three separate experiments were performed for each group.

2.6. Cell Invasion Assay. Cell invasion assays were performed by using the BD Matrigel Basement Membrane Matrix (BD Biosciences, New Jersey, USA) according to the manufacturer's instructions. The diluted Matrigel (1 : 5 ratio) was added to the upper chamber of a 24-well Transwell plate (Corning Company, New York, USA) and incubated at

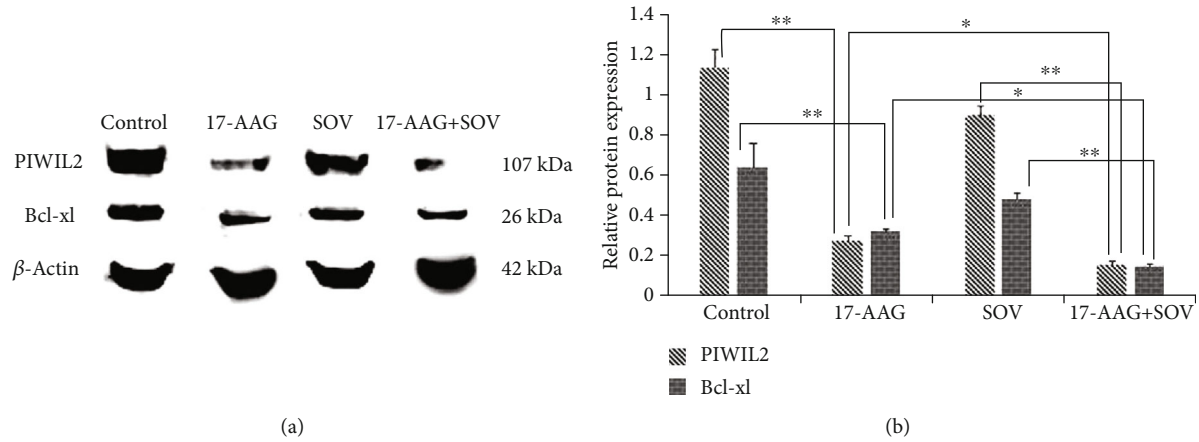

Figure 3: 5 μM 17-AAG, 5 μM SOV, and the mixture of 5 μM (17-AAG+SOV) reduce the expression of antiapoptotic protein at 72 h. (a) Western blot analysis of PIWIL2 and Bcl-xl protein level in SH-SY5Y cells. β-Actin was the loading control. (b) The bar graph showed the mean ± SD of the ratio interest proteins/β-actin band intensity obtained by pooling the results from 3 independent experiments in SH-SY5Y cells, respectively ($n = 3$, $^{*}P < 0.05$, $^{**}P < 0.01$).

37°C for 4-5 hours for gelling. Then, 2×10^5 SH-SY5Y cells in 100 μl DMEM serum-free medium were seeded into the upper compartment of the chamber, while 600 μl medium containing 20% FBS was added to the bottom compartment of the chamber. The drugs of 5 μM 17-AAG, 5 μM SOV, the mixture of 5 μM (17-AAG+SOV), or PBS were added into the upper chamber. Transwell plates were incubated at 37°C in a humidified atmosphere containing 5% CO_2 in air for 24 hours, and then, the noninvaded cells on the upper side of the chamber were wiped with cotton swabs. The cells that had migrated from the Matrigel into the pores of the inserted filter were fixed with 90% ethanol for 30 minutes and stained with 0.1% crystal violet dye for 10 min. The number of cells invading through the Matrigel was counted under an inverted microscope, and nine fields per well were counted. Each assay was repeated three times.

2.7. Statistical Analysis. All quantitative variables were expressed as the mean ± standard deviation (SD) and tested for normality using homogeneity variances prior to further statistical analysis. Each experiment was repeated three times. The data were analyzed by one-way ANOVA followed by Tukey's posttest using SPSS software, version 16.0. Differences were considered statistically significant at $P < 0.05$.

3. Results

3.1. 17-AAG Inhibits Cell Growth and Viability in SH-SY5Y Cells. To demonstrate the role of 17-AAG in NB, we investigated how 17-AAG affects cell viability in SH-SY5Y cells with different concentrations. After that, SH-SY5Y cells showed reduction in cell viability after 24 h of treatment with 5 μM 17-AAG, with a maximum reduction at 96 h (Figure 1). This antiviability effect was dose- and time-dependent at 1, 5, 10, and 25 μM at 48, 72 h, and 96 h. These results indicated that 17-AAG inhibits NB cell viability. Therefore, 5 μM 17-AAG was used for further assays.

3.2. 17-AAG Reduces the Percentage of Viable Cells. The flow chart showed that viable cells are located in the top left and dead cells are located in the lower right (Figure 2(a)). After 17-AAG treatment, the average percentages of viable cells were 85.13 ± 5.72, 76.63 ± 13.36, and 68.63 ± 1.10 at 24 h, 48 h, and 72 h, respectively, while those in the control group were 96.53 ± 1.15, 91.73 ± 6.95, and 90.73 ± 1.81, respectively (Figure 2(b), $^{*}P < 0.05$, $^{**}P < 0.01$). This suggested that 17-AAG could reduce the percentage of viable cells, especially at 72 h, about 24.3% (Figure 2(b)).

3.3. 17-AAG Reduces the Expression of PIWIL2 and Bcl-xl Proteins. Western blot was performed to determine if 5 μM 17-AAG inhibited the expression of PIWIL2 and Bcl-xl proteins in SH-SY5Y cells. The results showed that the expression of PIWIL2 and Bcl-xl proteins in SH-SY5Y cells reduced after treatment of 5 μM 17-AAG, 5 μM SOV, and the mixture of the two drugs (Figure 3(a)). In addition, the protein levels in the 5 μM (17-AAG+SOV) group reduced more than those in 5 μM 17-AAG or 5 μM SOV groups, which indicated that the combined effect is greater than the use of the single drug. Quantification analysis revealed the above results (Figure 3(b), $^{*}P < 0.05$, $^{**}P < 0.01$).

3.4. 17-AAG and SOV Treatment Induces Apoptosis in SH-SY5Y Cells. The early apoptotic cells could be stained by Annexin V, which is located in the right lower quadrant (Figure 4(a)). The results showed that 5 μM 17-AAG, 5 μM SOV, and the mixture of 5 μM (17-AAG+SOV) treatment increased the apoptotic rates of SH-SY5Y cells at 24 h, 48 h, and 72 h, compared with those in the control group ($^{*}P < 0.05$, $^{**}P < 0.01$, Figure 4(b)). In addition, the combined effect of 5 μM 17-AAG and 5 μM SOV was greater than the single use of any drug, and the apoptotic rates reached the climax at 48 h, then declined at 72 h (Figure 4(b)).

3.5. 17-AAG or SOV Treatment Inhibits the Invasion of SH-SY5Y Cells. SH-SY5Y cells that migrated into the lower

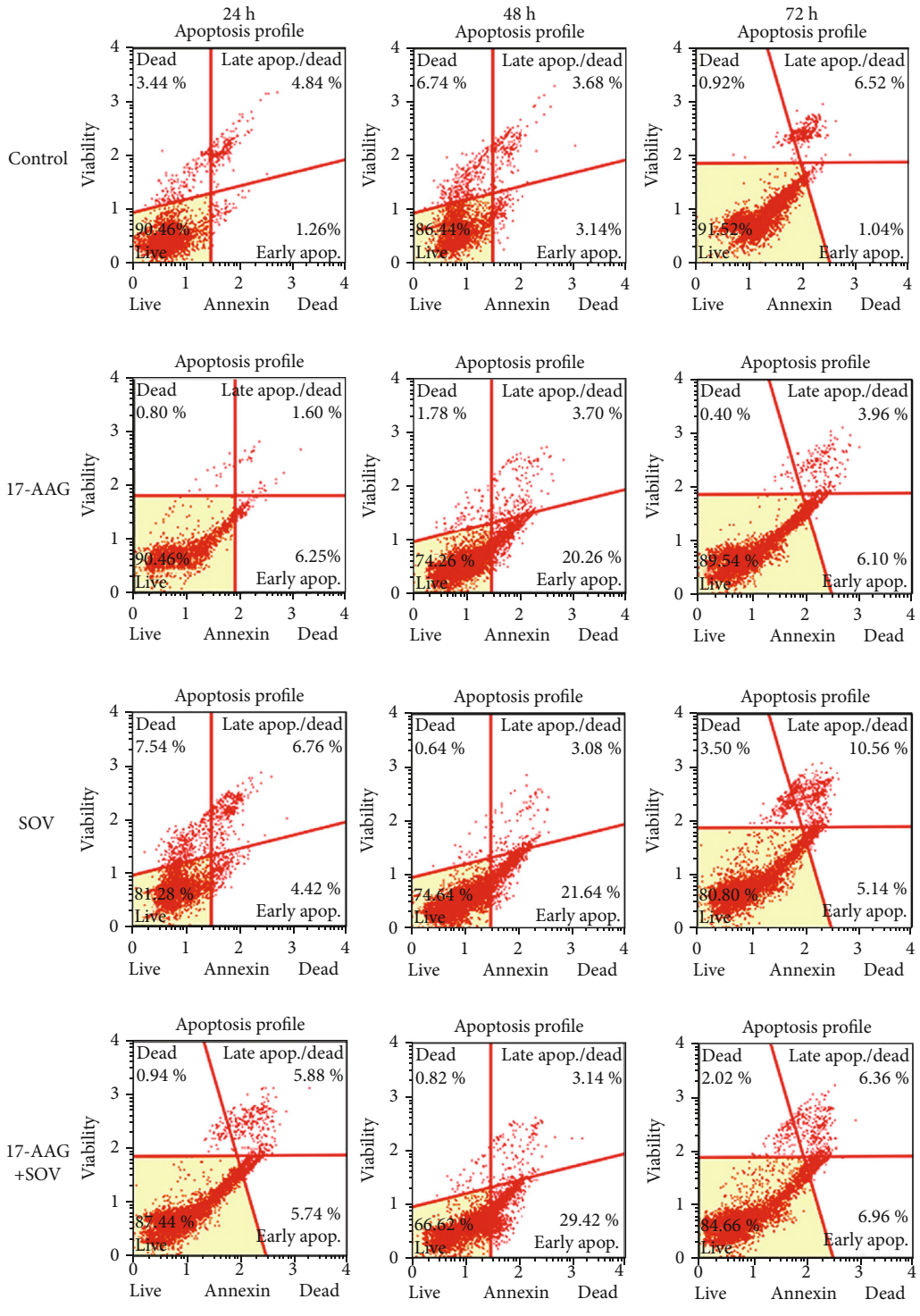

(a)

Figure 4: Continued.

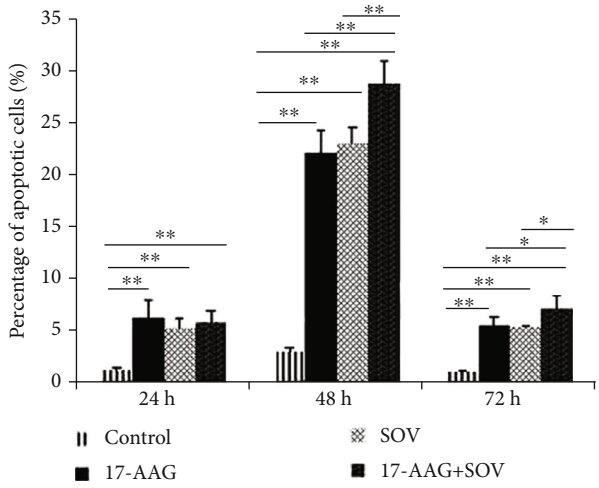

(b)

Figure 4: 5 μM 17-AAG, 5 μM SOV, and the mixture of 5 μM (17-AAG+SOV) induce cell apoptosis in SH-SY5Y cells. (a) The figures of SH-SY5Y cells stained with Annexin V in the control group, 5 μM 17-AAG group, 5 μM SOV group, and 5 μM (17-AAG+SOV) group. (b) The bar graph of the average percent of apoptotic cells in all groups ($n = 3$, $^{*}P < 0.05$, $^{**}P < 0.01$).

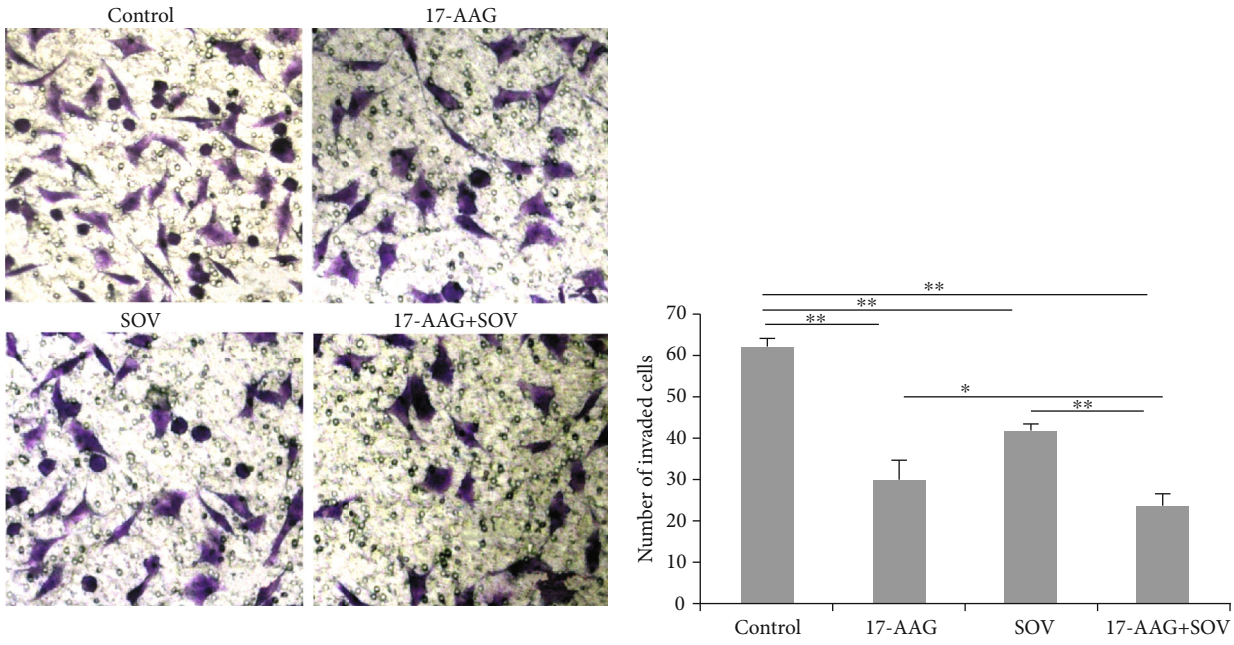

(a) (b)

Figure 5: 5 μM 17-AAG, 5 μM SOV, and 5 μM (17-AAG+SOV) inhibit the invasion of SH-SY5Y cells. (a) SH-SY5Y cells invaded into the bottom of the wells which were stained with crystal violet (×200). (b) Histogram of invaded SH-SY5Y cells in different groups. The bar graph of the relative expression of PIWIL2 mRNA in the control group and the SOV group ($n = 3$, $^{*}P < 0.05$, $^{**}P < 0.01$).

chamber were stained with crystal violet (Figure 5(a)). The results showed that amounts of migrated cells in the control, 5 μM 17-AAG, 5 μM SOV, and 5 μM (17-AAG+SOV) groups were 62.33 ± 2.08, 30.67 ± 4.02, 42.00 ± 2.00, and 23.67 ± 3.07, respectively, (Figure 5(b), $^{*}P < 0.05$, $^{**}P < 0.01$). After 5 μM 17-AAG, 5 μM SOV, or the mixture of 5 μM (17-AAG +SOV) treatment, the invasion rates decreased 50.8%, 32.6%, and 62.0%, respectively, compared with the control groups. It can be concluded that both 17-AAG and SOV treatment inhibited the invasion of SH-SY5Y cells, and the combined effect of them was greater than the single use of any drug.

4. Discussion

Here, we describe the effects of 17-AAG used alone or in combination with SOV on apoptosis and invasion of SH-

SY5Y cells and explore the level of PIWIL2 expression as a promising mechanism. Our research has achieved certain results and provided a therapeutic strategy for the treatment of tumors.

HSP90 is a molecular chaperone required for the stability and function of many proteins. The survival, growth, and invasive potential of cancer cells can be enhanced by HSP90. And HSP90 inhibitors are promising new anticancer agents, among which 17-AAG is in clinical evaluation now [30]. 17-AAG has exhibited lower toxicity and improved stability and induced reduction of key regulators of signal transduction in many human tumors, including colon and breast cancers [31, 32].

In our study, we found that 17-AAG inhibited cell growth and viability in SH-SY5Y cells at different concentrations (Figure 1). When we treated SH-SY5Y cells with 5 μM 17-AAG, the cells' viability reduced sharply at 24, 48, 72, and 96 h (Figure 1). So, we used this concentration for further tests. The results of apoptosis and invasion assay showed that the single use of 17-AAG or SOV induced significant apoptosis and inhibited the invasion in SH-SY5Y cells at 24 h, 48 h, and 72 h, compared with those in the control groups (Figures 4 and 5). And the combined use of the two drugs had a more significant effect than the single use of any drug, which demonstrated that 17-AAG and SOV have a synergistic inhibitory effect on SH-SY5Y cell development. The antitumor effects of 17-AAG or SOV were demonstrated in multiple studies [14, 19, 24], and our study confirmed the advantages of their combined usage.

It has been reported that PIWI proteins played a role in germ cell proliferation, differentiation, germline stem cell maintenance, and transposon control in germline from Drosophila to mammals. The PIWIL2 gene is mainly expressed in the testis or embryonic cells among normal tissues but widely expressed in tumors [33, 34]. Increasing evidence has proven that PIWI proteins are linked to the hallmarks of cancer, such as cell proliferation, antiapoptosis, and invasion. This provides new possibilities for anticancer therapies through the targeting of PIWI proteins [35, 36]. Bcl-xl is one of the leading members of the Bcl-2 protein family and exerts its antiapoptotic role to mediate the interaction with the proapoptotic members of the same Bcl-2 family [37, 38]. Lee et al. demonstrated that PIWIL2 inhibited apoptosis and stimulated proliferation through activation of Stat3/Bcl-xl and enhancement of Stat3/cyclin D1 signaling pathways [39, 40]. In our previous studies, we have known that SOV inhibited the growth of SH-SY5Y cells via the piRNA-PIWI signal, which is consistent with the report of Izumi et al. in the silkworm ovary-derived BmN4 cells [41]. Then, we want to verify if 17-AAG can enhance this effect. The result of Western blot showed that the expression of PIWIL2 and Bcl-xl proteins reduced when treated with 17-AAG, SOV, and the mixture of the two drugs (Figure 3). Besides, the result of the apoptosis assay showed that the single use of 17-AAG or SOV induced significant apoptosis in SH-SY5Y cells at 24 h, 48 h, and 72 h, compared with those in the control groups (Figure 4). And the combined use of the two drugs had more significant effect than the single use of any drug, which demonstrated that 17-AAG could enhance the apoptosis effect induced by SOV in SH-SY5Y cells. In addition, the invasion assay showed that 17-AAG or SOV treatment inhibited the invasion of SH-SY5Y cells, compared with control groups, and the combined use of the two drugs had greater effect than the single use of any drug (Figure 5). Therefore, we speculated that 17-AAG plays its role by modulating PIWIL2 via the piRNA-PIWI signal pathway.

The limitations of this study may include the mechanism of molecular action which remains to be further studied. In addition, we have only conducted *in vitro* experiments, and *in vivo* and clinical trials are essential if clinical transformation is to be achieved. Furthermore, there are some shortcomings in 17-AAG itself. At present, it is mainly improved by combining nanomaterials [42, 43], and related researches can be carried out in the later stage. Despite the fact that this study is preliminary, we clearly indicated that 17-AAG used as a single agent or combined with SOV had antineoplastic effect on SH-SY5Y, which may offer a new strategy to treat neuroblastoma or other central nervous system tumors/diseases.

5. Conclusions

In conclusion, 17-AAG can promote apoptosis and inhibit invasion of SH-SY5Y cells. Furthermore, a synergistic inhibitory effect of 17-AAG combined with SOV has been shown on SH-SY5Y cells. This synergistic effect was mediated through induction of apoptosis by downregulating PIWIL2-related pathways.

Data Availability

Readers can access all the data supporting the conclusions of the study online.

Conflicts of Interest

All authors declare that there is no conflict of interest regarding the publication of this article.

Authors' Contributions

Xiaohong Tian designed and wrote the main content. Wumei Wei, Xiaohong Wang, Jun Fan, Weijian Hou, Shuling Bai, and Hao Tong contributed some detailed techniques (e.g., data analysis and interpretation) and revised the manuscript. Qiang Ao revised the manuscript. Xiaohong Tian conceived, allocated, and revised the manuscript. All authors have read and agreed to the published version of the manuscript.

Acknowledgments

The work was supported by grants from the National Natural Science Foundation of China (NSFC) (Nos. 31600793 and 81571832).

References

[1] H. Shimada, I. M. Ambros, L. P. Dehner, J. Hata, V. V. Joshi, and B. Roald, "Terminology and morphologic criteria of neuroblastic tumors: recommendations by the International Neuroblastoma Pathology Committee," *Cancer*, vol. 86, no. 2, pp. 349–363, 1999.

[2] T. A. Ishola and D. H. Chung, "Neuroblastoma," *Surgical Oncology*, vol. 16, no. 3, pp. 149–156, 2007.

[3] S. E. Sharp, M. J. Gelfand, and B. L. Shulkin, "Pediatrics: diagnosis of neuroblastoma," *Seminars in Nuclear Medicine*, vol. 41, no. 5, pp. 345–353, 2011.

[4] A. D. Pearson, C. R. Pinkerton, I. J. Lewis, J. Imeson, C. Ellershaw, and D. Machin, "High-dose rapid and standard induction chemotherapy for patients aged over 1 year with stage 4 neuroblastoma: a randomised trial," *The Lancet Oncology*, vol. 9, no. 3, pp. 247–256, 2008.

[5] P. E. Zage, M. Kletzel, K. Murray et al., "Outcomes of the POG 9340/9341/9342 trials for children with high-risk neuroblastoma: a report from the Children's Oncology Group," *Pediatric Blood & Cancer*, vol. 51, no. 6, pp. 747–753, 2008.

[6] J. Kang, A. Kamal, F. J. Burrows, B. M. Evers, and D. H. Chung, "Inhibition of neuroblastoma xenograft growth by Hsp90 inhibitors," *Anticancer Research*, vol. 26, no. 3A, pp. 1903–1908, 2006.

[7] J. Korbecki, I. Baranowska-Bosiacka, I. Gutowska, and D. Chlubek, "Biochemical and medical importance of vanadium compounds," *Acta Biochimica Polonica*, vol. 59, no. 2, pp. 195–200, 2012.

[8] J. Namkaew, T. Jaroonwitchawan, N. Rujanapun, J. Saelee, and P. Noisa, "Combined effects of curcumin and doxorubicin on cell death and cell migration of SH-SY5Y human neuroblastoma cells," *In vitro Cellular & Developmental Biology Animal*, vol. 54, no. 9, pp. 629–639, 2018.

[9] S. S. Hussain, K. Rafi, S. Faizi, Z. A. Razzak, and S. U. Simjee, "A novel, semi-synthetic diterpenoid 16(R and S)-phenylamino-cleroda-3,13(14), Z-dien-15,16 olide (PGEA-AN) inhibits the growth and cell survival of human neuroblastoma cell line SH-SY5Y by modulating P53 pathway," *Molecular and Cellular Biochemistry*, vol. 449, no. 1-2, pp. 105–115, 2018.

[10] L. M. de Medeiros, M. A. De Bastiani, E. P. Rico et al., "Cholinergic differentiation of human neuroblastoma SH-SY5Y cell line and its potential use as an in vitro model for Alzheimer's disease studies," *Molecular Neurobiology*, vol. 56, no. 11, pp. 7355–7367, 2019.

[11] H. Xicoy, B. Wieringa, and G. J. Martens, "The SH-SY5Y cell line in Parkinson's disease research: a systematic review," *Molecular Neurodegeneration*, vol. 12, no. 1, p. 10, 2017.

[12] A. Krishna, M. Biryukov, C. Trefois et al., "Systems genomics evaluation of the SH-SY5Y neuroblastoma cell line as a model for Parkinson's disease," *BMC Genomics*, vol. 15, no. 1, p. 1154, 2014.

[13] J. G. Supko, R. L. Hickman, M. R. Grever, and L. Malspeis, "Preclinical pharmacologic evaluation of geldanamycin as an antitumor agent," *Cancer Chemotherapy and Pharmacology*, vol. 36, no. 4, pp. 305–315, 1995.

[14] S. Talaei, H. Mellatyar, A. Asadi, A. Akbarzadeh, R. Sheervalilou, and N. Zarghami, "Spotlight on 17-AAG as an Hsp90 inhibitor for molecular targeted cancer treatment," *Chemical Biology & Drug Design*, vol. 93, no. 5, pp. 760–786, 2019.

[15] X.-. Y. Ye, Q.-. Q. Luo, Y.-. H. Xu et al., "17-AAG suppresses growth and invasion of lung adenocarcinoma cells via regulation of the LATS1/YAP pathway," *Journal of Cellular and Molecular Medicine*, vol. 19, no. 3, pp. 651–663, 2015.

[16] J. L. Roh, E. H. Kim, H. B. Park, and J. Y. Park, "The Hsp90 inhibitor 17-(allylamino)-17-demethoxygeldanamycin increases cisplatin antitumor activity by inducing p53-mediated apoptosis in head and neck cancer," *Cell Death & Disease*, vol. 4, no. 12, article e956, 2013.

[17] Z. Zhang, Z. Xie, G. Sun et al., "Reversing drug resistance of cisplatin by hsp90 inhibitors in human ovarian cancer cells," *International Journal of Clinical and Experimental Medicine*, vol. 8, no. 5, pp. 6687–6701, 2015.

[18] Y. Wu, Y. Ma, Z. Xu et al., "Sodium orthovanadate inhibits growth of human hepatocellular carcinoma cells in vitro and in an orthotopic model in vivo," *Cancer Letters*, vol. 351, no. 1, pp. 108–116, 2014.

[19] W. Jiang, G. Li, W. Li et al., "Sodium orthovanadate overcomes sorafenib resistance of hepatocellular carcinoma cells by inhibiting Na(+)/K(+)-ATPase activity and hypoxia-inducible pathways," *Scientific Reports*, vol. 8, no. 1, p. 9706, 2018.

[20] Q. Yu, W. Jiang, D. Li et al., "Sodium orthovanadate inhibits growth and triggers apoptosis of human anaplastic thyroid carcinoma cells *in vitro* and *in vivo*," *Oncology Letters*, vol. 17, no. 5, pp. 4255–4262, 2019.

[21] A. A. Khalil and M. J. Jameson, "Sodium orthovanadate inhibits proliferation and triggers apoptosis in oral squamous cell carcinoma in vitro," *Biochemistry Biokhimiia*, vol. 82, no. 2, pp. 149–155, 2017.

[22] H. Izumi, H. Touge, T. Igishi et al., "Favorable effect of the combination of vinorelbine and dihydropyrimidine dehydrogenase-inhibitory fluoropyrimidine in EGFR-mutated lung adenocarcinoma: retrospective and in vitro studies," *International Journal of Oncology*, vol. 46, no. 3, pp. 989–998, 2015.

[23] T. M. F. Günther, M. R. Kviecinski, C. C. Baron et al., "Sodium orthovanadate associated with pharmacological doses of ascorbate causes an increased generation of ROS in tumor cells that inhibits proliferation and triggers apoptosis," *Biochemical and Biophysical Research Communications*, vol. 430, no. 3, pp. 883–888, 2013.

[24] A. Morita, S. Yamamoto, B. Wang et al., "Sodium orthovanadate inhibits p53-mediated apoptosis," *Cancer Research*, vol. 70, no. 1, pp. 257–265, 2010.

[25] A. M. Kordowiak, A. Goc, E. Drozdowska, B. Turyna, and W. Dabros, "Sodium orthovanadate exerts influence on liver Golgi complexes from control and streptozotocin-diabetic rats," *Journal of Inorganic Biochemistry*, vol. 99, no. 5, pp. 1083–1089, 2005.

[26] M. Sun, H. Izumi, Y. Shinoda, and K. Fukunaga, "Neuroprotective effects of protein tyrosine phosphatase 1B inhibitor on cerebral ischemia/reperfusion in mice," *Brain Research*, vol. 1694, pp. 1–12, 2018.

[27] X. Tian, J. Fan, W. Hou, S. Bai, Q. Ao, and H. Tong, "Sodium orthovanadate induces the apoptosis of SH-SY5Y cells by inhibiting PIWIL2," *Molecular Medicine Reports*, vol. 13, no. 1, pp. 874–880, 2016.

[28] J. J. Ipsaro, A. D. Haase, S. R. Knott, L. Joshua-Tor, and G. J. Hannon, "The structural biochemistry of Zucchini implicates it as a nuclease in piRNA biogenesis," *Nature*, vol. 491, no. 7423, pp. 279–283, 2012.

[29] Y. Cheng, Q. Wang, W. Jiang et al., "Emerging roles of piRNAs in cancer: challenges and prospects," *Aging*, vol. 11, no. 21, pp. 9932–9946, 2019.

[30] X. Liu, L. L. Ban, G. Luo et al., "Acquired resistance to HSP90 inhibitor 17-AAG and increased metastatic potential are associated with MUC1 expression in colon carcinoma cells," *Anti-Cancer Drugs*, vol. 27, no. 5, pp. 417–426, 2016.

[31] S. Z. Usmani and G. Chiosis, "HSP90 inhibitors as therapy for multiple myeloma," *Clinical Lymphoma, Myeloma & Leukemia*, vol. 11, Supplement 1, pp. S77–S81, 2011.

[32] R. Schulz, N. D. Marchenko, L. Holembowski et al., "Inhibiting the HSP90 chaperone destabilizes macrophage migration inhibitory factor and thereby inhibits breast tumor progression," *The Journal of Experimental Medicine*, vol. 209, no. 2, pp. 275–289, 2012.

[33] Y. Lu, K. Zhang, C. Li et al., "Piwil2 suppresses p53 by inducing phosphorylation of signal transducer and activator of transcription 3 in tumor cells," *PLoS One*, vol. 7, no. 1, article e30999, 2012.

[34] W. Li, J. Martinez-Useros, N. Garcia-Carbonero et al., "The prognosis value of PIWIL1 and PIWIL2 expression in pancreatic cancer," *Journal of Clinical Medicine*, vol. 8, no. 9, p. 1275, 2019.

[35] Y. Tan, L. Liu, M. Liao et al., "Emerging roles for PIWI proteins in cancer," *Acta Biochimica et Biophysica Sinica*, vol. 47, no. 5, pp. 315–324, 2015.

[36] A. A. Mentis, E. Dardiotis, N. A. Romas, and A. G. Papavassiliou, "PIWI family proteins as prognostic markers in cancer: a systematic review and meta-analysis," *Cellular and Molecular Life Sciences*, vol. 77, no. 12, pp. 2289–2314, 2020.

[37] C. Gabellini, D. Trisciuoglio, and D. Del Bufalo, "Non-canonical roles of Bcl-2 and Bcl-xL proteins: relevance of BH4 domain," *Carcinogenesis*, vol. 38, no. 6, pp. 579–587, 2017.

[38] A. V. Follis, F. Llambi, H. Kalkavan et al., "Regulation of apoptosis by an intrinsically disordered region of Bcl-xL," *Nature Chemical Biology*, vol. 14, no. 5, pp. 458–465, 2018.

[39] J. H. Lee, D. Schütte, G. Wulf et al., "Stem-cell protein Piwil2 is widely expressed in tumors and inhibits apoptosis through activation of Stat3/Bcl-XL pathway," *Human Molecular Genetics*, vol. 15, no. 2, pp. 201–211, 2006.

[40] B. C. O'Connell, K. O'Callaghan, B. Tillotson et al., "HSP90 inhibition enhances antimitotic drug-induced mitotic arrest and cell death in preclinical models of non-small cell lung cancer," *PLoS One*, vol. 9, no. 12, article e115228, 2014.

[41] N. Izumi, S. Kawaoka, S. Yasuhara et al., "Hsp90 facilitates accurate loading of precursor piRNAs into PIWI proteins," *RNA*, vol. 19, no. 7, pp. 896–901, 2013.

[42] H. Mellatyar, S. Talaei, Y. Pilehvar-Soltanahmadi et al., "17-DMAG-loaded nanofibrous scaffold for effective growth inhibition of lung cancer cells through targeting HSP90 gene expression," *Biomedicine & Pharmacotherapy*, vol. 105, pp. 1026–1032, 2018.

[43] M. Dadashpour, Y. Pilehvar-Soltanahmadi, S. A. Mohammadi et al., "Watercress-based electrospun nanofibrous scaffolds enhance proliferation and stemness preservation of human adipose-derived stem cells," *Artificial Cells, Nanomedicine, and Biotechnology*, vol. 46, no. 4, pp. 819–830, 2018.